A Novel Checkerboard Metasurface Based on Optimized Multielement Phase Cancellation for Superwideband RCS Reduction

Jianxun Su, Yao Lu, Jiayi Liu, Yaoqing Yang, *Senior Member, IEEE*, Zengrui Li, *Member, IEEE* and Jiming Song, *Fellow, IEEE*

***Abstract*— In this paper, a checkerboard metasurface based on a novel physical mechanism, optimized multielement phase cancellation, is proposed for greatly expanding the bandwidth of radar cross section (RCS) reduction. More basic metaparticles and, in particular, the variable phase difference between them, greatly increase the ability to control electromagnetic waves. Interactions between multiple local waves produced by the basic metaparticles at multiple frequencies sampled in a superwide frequency band are manipulated and optimized simultaneously to achieve phase cancellation. The proposed metasurface can achieve a 10 dB RCS reduction in a superwide frequency band from 5.5 to 32.3 GHz with a ratio bandwidth (f_H/f_L) of 5.87:1 under normal incidence for both polarizations. Furthermore, the RCS reduction is larger than 8 dB from 5.4 to 40 GHz with a ratio bandwidth of 7.4:1. The metasurface also has a good performance under wide-angle oblique incidences. The optimal metaparticle distribution is found to obtain the superwideband bistatic RCS reduction. The theoretical analysis, simulation, and experimental results are in good agreement and verify the ability and capability of the proposed mechanism.**

***Index Terms*— Metasurface, optimized multielement phase cancellation (OMEPC), radar cross section (RCS) reduction, superwideband.**

I. Introduction

METAMATERIALS and metasurfaces are artificial structures designed for controlling electromagnetic (EM) and acoustic waves or fields. With their rapid development in recent years, scholars are paying more attention to various novel structures and the exceptional, unexpected physical properties in addition to the effective medium parameters [1]. These properties lead to some fascinating phenomena, such as negative refraction [2], subwavelength imaging [3], field enhancement [4], and anomalous tunneling effects [5]. Novel devices based on these ideas, such as ultrathin metalenses or perfect lenses [6], invisibility cloak [7]–[9], plasmonic waveguide [10], and polarization converter [11], have been fabricated and tested over the past few years. One of the potential applications of metasurfaces is to reduce the scattering field of a metal object.

To effectively reduce the radar cross section (RCS) of the target is challenging. Four approaches are usually used to reduce the RCS of a target in electromagnetism. The first approach is to apply a frequency-selective surface or a metamaterial absorber, which transform the EM energy into heat [12]–[14]. However, broadband impedance matching for radar absorbing is hard to achieve. The second approach is to alter the appearance of the target (shaping) to reduce the scattered field along source directions but that may destroy the aerodynamic layout and increase the complexity of the shape design [15], [16]. The third approach is the use of transformation electromagnetics and optics [7]–[9]. EM waves propagate around the target surface, and the backscattered field is suppressed. The last approach is the opposite phase cancellation (OPC). As an effective method of suppressing the vector fields, it has been widely used in the fields of electromagnetics, optics, and acoustics [17]–[20].

OPC is a traditional method of achieving the RCS reduction. The basic idea is to exploit the cancellation effects arising from the well-known 180° phase difference between the corresponding reflection coefficients. Since the frequency and direction of incoming waves are unpredictable in reality, the bandwidth and oblique incidence performance are two important factors of stealth technology. Based on a combination of artificial magnetic conductors (AMCs) and perfect electric conductors (PECs) in a chessboardlike configuration, Paquay *et al.* [21] proposed a planar structure for RCS reduction. The backscattered field can be effectively cancelled by redirecting it along with other angles. However, the narrow in-phase reflection bandwidth of the AMC restricts the RCS reduction frequency range. In [22], a planar monolayer

Manuscript received January 17, 2018; revised July 21, 2018; accepted July 22, 2018. Date of publication September 17, 2018; date of current version November 30, 2018. This work was supported in part by the National Natural Science Foundation of China under Grant 61671415 and Grant 61701448 and in part by the Key Projects of Engineering Planning of Communication University of China under Grant 3132016XNG1604. *(Corresponding author: Zengrui Li.)*

J. Su is with the School of Information Engineering, Communication University of China, Beijing 100024, China, and also with the Science and Technology on Electromagnetic Scattering Laboratory, Beijing 100854, China (e-mail: sujianxun_jlgx@163.com).

Y. Lu, J. Liu, and Z. Li are with the School of Information Engineering, Communication University of China, Beijing 100024, China (e-mail: zrli@cuc.edu.cn).

Y. Yang is with the Department of Electrical and Computer Engineering, University of Nebraska–Lincoln, Lincoln, NE 68182 USA.

J. Song is with the Department of Electrical and Computer Engineering, Iowa State University, Ames, IA 50011 USA, and also with the School of Information Engineering, Communication University of China, Beijing 100024, China (e-mail: jisong@iastate.edu).

Color versions of one or more of the figures in this paper are available online at http://ieeexplore.ieee.org.

Digital Object Identifier 10.1109/TAP.2018.2870372

chessboard structure is presented for broadband RCS reduction using AMC technology. Fractional bandwidth (FBW) of more than 40% is obtained with a monostatic RCS reduction larger than 10 dB. These rectangular checkerboard surfaces of periodic phase arrangement create four scattering beams and the bistatic RCS reduction of about 8.1 dB [21]–[24]. Chen *et al.* [25] proposed a hexagonal checkerboard surface of periodic phase arrangement, with a 10 dB monostatic RCS reduction bandwidth of about 61%, which can create six bistatic RCS lobes, leading to further bistatic RCS reduction. A chessboard AMC surface composed of saltire arrow and four-E-shaped unit cells has a bandwidth of 85% for 10 dB RCS reduction [26]. Then, the dual-wideband checkerboard surfaces are presented in [27], and the bandwidths of 10 dB RCS reduction in the frequency bands of 3.94–7.40 GHz and 8.41–10.72 GHz are about 61% and 24% by utilizing two dual-band EM bandgap structures. Haji-Ahmadi *et al.* [28] proposed a pixelated checkerboard metasurface for ultrawideband RCS reduction. Two unit cells are designed based on the pixelation and optimization of a square patch and achieve 95% measured bandwidth for 10 dB RCS reduction. In [29], the polarization conversion metasurface is utilized to realize a wideband RCS reduction. Phase differences of cross-polarized field components between the polarization conversion element and its mirror element are exactly 180°, resulting in OPC. In [30], the metasurface, composed of square- and L-shaped patches, can convert the polarization of the incident wave to its cross-polarized direction. A 10 dB RCS reduction is achieved over an ultrawideband of 98%.

Recently, coding and digital metamaterials have been proposed for wideband RCS reduction through the design of coding sequences using digital elements "0" and "1," which possess opposite phase responses [31]–[33]. RCS reduction is essentially based on OPC. In [31], 1 bit and 2 bit coding metasurfaces composed of digital elements were proposed, and the 10 dB RCS reduction bandwidth of 66.67% was achieved. A 3 bit coding metasurface based on multiresonant polarization conversion elements was presented in [32]. The bandwidth of 10 dB RCS reduction was 89.9%. A broadband and broad-angle polarization-independent, random-coding metasurface for RCS reduction has been proposed in [33]. The 10 dB RCS reduction bandwidth of 84.75% was realized.

The previous research focused mainly on the design of unit cells with a fixed phase difference of approximately 180° for OPC or coding metamaterials. However, bandwidth expansion for RCS reduction is extremely difficult. This paper was aimed at breaking the bandwidth constraints of OPC and coding metamaterial.

Our research is focused primarily on the development of novel phase cancellation methods. A metasurface based on the new physical mechanism of optimized multielement phase cancellation (OMEPC) is proposed for superwideband RCS reduction. More basic metaparticles and variable phase differences between them greatly enhance the ability to achieve phase cancellation. Superwideband manipulation of multiple EM waves is realized by adjusting the side length of the square ring patch and the thickness of the dielectric layer of the basic metaparticles. The geometric parameters of the basic metaparticles are optimized and determined by the field superposition principle and particle swarm optimization (PSO) algorithm to achieve good RCS reduction in a superwide frequency band. The metasurface can achieve more than 10 dB RCS reduction in a superwide frequency band ranging from 5.5 to 32.3 GHz with a ratio bandwidth (f_H/f_L) of 5.87:1 under normal incidence for both polarizations. Furthermore, the RCS reduction is larger than 8 dB from 5.4 to 40 GHz with a ratio bandwidth of 7.4:1. The metasurface also has an excellent performance under wide-angle oblique incidences. The analysis, simulation, and measurement results demonstrate that our proposed physical mechanism greatly expands the RCS reduction bandwidth.

This paper has been structured as follows. The novel physical mechanism, OMEPC, is introduced in Section II. Section III describes the design process of the superwideband RCS reducer metasurface in detail in three steps. The simulations and measurements of the monostatic and bistatic scattering characteristic for normal and oblique incidences are discussed in Section IV. Finally, the conclusions are summarized in Section V.

II. Optimized Multielement Phase Cancellation

The phenomenon of interference between waves is based on the field superposition principle. When two or more waves from different local areas of a metasurface travel into the same space, the net amplitude at each point is the sum of the amplitudes of the individual waves. A metasurface consists of a 2-D array of $M \times N$ tiles, which are uniformly spaced with d_x in the x-direction and d_y in the y-direction, as shown in Fig. 1(a). Based on planar array theory, the scattering field $E^s(\theta, \varphi)$ of the metasurface under normal incidence can be synthesized accurately by [34]

$$E^S = \mathrm{EP} \times \mathrm{AF} \tag{1}$$

where EP is the pattern function of a tile, which is fixed in our model. AF represents the array factor, which can be described as

$$\begin{aligned}\mathrm{AF}(\theta,\varphi) &= \sum_{m=1}^{M}\sum_{n=1}^{N} A_{m,n}\exp\left\{j\left[2\pi\sin\theta\left(\cos\varphi\cdot md_x+\sin\varphi\cdot nd_y\right)\right.\right.\\ &\qquad \left.\left./\lambda+\phi_{m,n}\right]\right\}\end{aligned} \tag{2}$$

where θ and φ are the elevation angle and azimuth angle of an arbitrary scattering direction, respectively. $\Gamma_{m,n} = A_{m,n}e^{j\emptyset_{m,n}}$ is the reflection coefficient of the (m, n)th basic tile. Especially in the backward direction, array factor is simplified to

$$\mathrm{AF}(0,\varphi) = \sum_{m=1}^{M}\sum_{n=1}^{N} A_{m,n}e^{j\phi_{m,n}}. \tag{3}$$

It is worth noting that the backscattering field is independent of the tile arrangement but only dependent on their reflection coefficients.

The RCS reduction (σ_R) of the metasurface, compared to an equal-sized PEC surface, can be represented

by [25]

$$\sigma_R = 10\log\frac{|E^s|^2}{|E^i|^2} \tag{4}$$

where E^i is the incident electric field.

For a multielement checkerboard surface with $P(=M \cdot N)$ tiles, the RCS reduction can be derived based on (5) in [25], which can be approximated by

$$\sigma_R = 10\log\left|\frac{\mathrm{AF}(0,\varphi)}{P}\right|^2 = 10\log\left|\frac{\sum_{i=1}^{P} A_i e^{j\phi_i}}{P}\right|^2. \tag{5}$$

Equation (5) does not include the coupling between the tiles and edge effect but provides a good guideline for RCS reduction of the metasurface compared to an equal-sized PEC surface.

The reflection amplitudes are unity ($A_1 \approx A_2 \approx \ldots A_P \approx 1$) due to a lossless ground surface. To achieve a 10 dB RCS reduction, the reflection phases of basic metaparticles need to satisfy the following relationship:

$$\left|\sum_{i=1}^{P} e^{j\phi_i}\right| \le P\sqrt{0.1} \tag{6}$$

which is a multivariate exponential inequality. Completely phase cancellation requires

$$\left|\sum_{i=1}^{P} e^{j\phi_i}\right| = 0 \tag{7}$$

which is an exponential indefinite equation. It is noted that (6) and (7) have many solutions. Obviously, OPC and coding metamaterials are just two special solutions. However, more solutions will be excluded. For OPC and coding metamaterials, due to the fixed number of unit cells and the fixed phase difference between them, the ability to realize phase cancellation is greatly reduced, leading to a narrow bandwidth of RCS reduction.

Here, a metasurface based on a new physical mechanism of OMEPC is proposed for superwideband RCS reduction. Multiple reflected waves are superimposed in space to achieve phase cancellation, as shown in Fig. 1(b). The phase control of the basic metaparticles is arbitrary. More basic metaparticles and, in particular, variable phase difference between them greatly increase the ability to achieve superwideband phase cancellation. The design process of the metasurface for superwideband RCS reduction is divided into the following three steps:

1) *Unit Cell and Its Reflection Characteristics:* The choice of unit cell shape should satisfy that reflection phase range with the change of some geometric parameters of a unit cell is large enough in a superwide frequency band. This phase feature guarantees the superwideband manipulation of EM waves.
2) *Optimization Design of Basic Metaparticles:* This is the most important step. From (3), we know that the backscattering field is only related to the reflection phase of the basic metaparticles but independent of their distribution under normal incidence. OMEPC combining (5) and PSO algorithm is used to optimize and determine the geometric parameters of basic metaparticles, which can obtain the maximum bandwidth for the monostatic/backward RCS reduction.
3) *Surface Metaparticle Layout:* Based on planar array theory, random metaparticle distributions were performed to find the optimal surface phase layout for diffuse scattering of EM waves in a superwide frequency band, leading to a low bistatic RCS simultaneously.

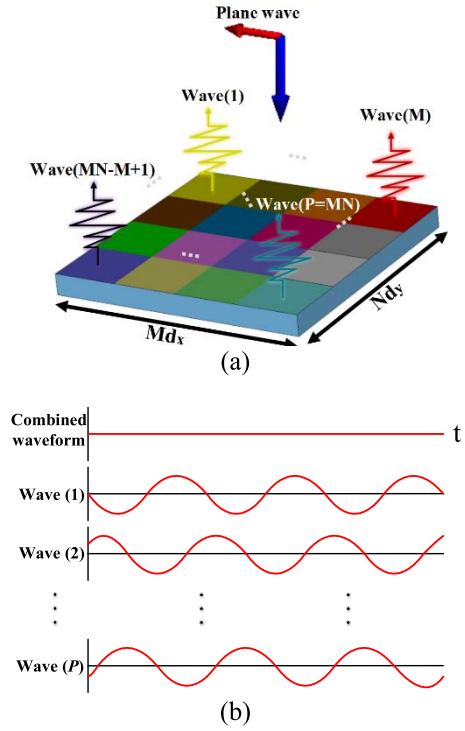

Fig. 1. Plane wave incident on a metasurface consisted of $P(=M \times N)$ tiles. (a) P scattering waves with a different reflection phase were produced locally by the tiles. (b) Combined waveform in the far field is the superposition of these P scattering waves.

III. Metasurface Design

In this section, the design process of the superwideband RCS reducer metasurface is described in three steps.

A. Unit Cell and Its Reflection Characteristics

The square ring patch was chosen as the basic metaparticle of the metasurface for its reflection phase change characteristics. The range of reflection phase changing with side length is large enough in a superwide frequency band. The unit cells were printed on the surface of polytetrafluoroethylene woven glass (Model: F4B-2, Wangling Insulating Materials, Taizhou, China) substrate with a dielectric constant $\varepsilon_r = 2.65$ and loss tangent $\tan\delta = 0.001$. The back of the substrate is a PEC ground plane. The geometry structure of the basic metaparticle is illustrated in Fig. 2(a). The basic metaparticles were simulated by frequency domain solver (finite element method) of CST Microwave Studio. The periodic boundary condition (PBC) is imposed on unit cells to create infinite

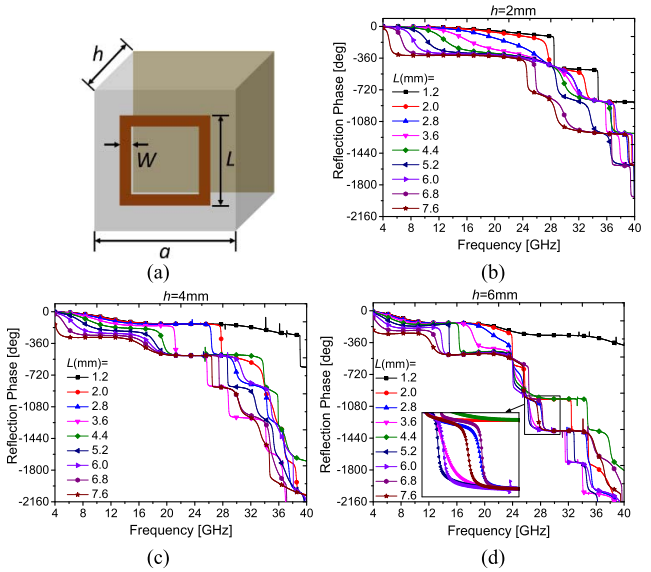

Fig. 2. Geometry of the basic metaparticle and its reflection phase properties. (a) Geometry structure of the square ring element. Dimensions: $a = 8$ mm, $w = 0.4$ mm, $h = 2$, 4, and 6 mm. (b)–(d) Reflection phase of basic metaparticles with the change of side length L of square rings for the dielectric layer thickness of 2, 4, and 6 mm, respectively.

structure and obtain their reflection coefficients. In this simulation, side length L of the metaparticles varied from 1.2 to 7.6 mm with a step size of 0.02 mm, while there were three choices of layer thickness for the dielectric substrate: 2, 4, and 6 mm. The layer thickness includes the copper layer thickness of 0.035 mm×2 mm on both sides. The periodicity a of the unit cell and the width w of the square ring were fixed. To fix the reference plane where the phase is obtained, in the CST model, a small patch with material "vaccum" is always set at the plane ($z = 7$ mm). A part of the reflection phase curves is plotted in Fig. 2(b)–(d), respectively. The phase changes drastically in some frequencies, as shown in the partial enlargement of Fig. 2(d). The available phase coverage by tuning the side length of the square ring and dielectric layer thickness was larger than 250° at frequencies ranging from 5 to 28 GHz. This phase feature guarantees the possibility of superwideband manipulation of EM waves.

B. Optimization Design of Basic Metaparticles

In this paper, the RCS reducer metasurface consisted of 4×4 tiles. Each tile was a subarray of basic metaparticle, i.e., the number of basic metaparticles was $P = 16$. Effective manipulation of EM waves in an ultrawide frequency band by adjusting the geometric parameter of the basic metaparticles was first proposed and proved in [35]. The schematic for superwideband control of RCS reduction by adjusting the side length of the square ring and the thickness of dielectric layer is depicted in Fig. 3, where Q is the number of optimization frequencies ($f_1, f_2, \ldots f_Q$). The reflection phase versus frequency plotted in Fig. 2 was prestored in a table. For P basic metaparticles, $P \times Q$ phase values can be read from the reflection phase table. These $P \times Q$ phase values resulted in Q values of RCS reduction at Q optimization frequencies. Finally, these Q values were used to evaluate the

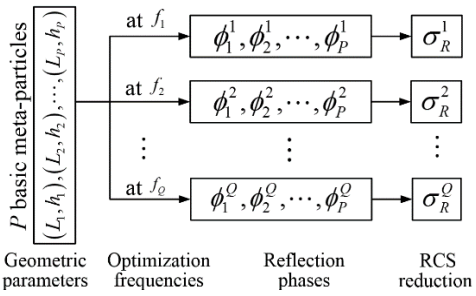

Fig. 3. Schematic of the superwideband manipulation of RCS reduction by geometric parameter adjustment. The side length L and the dielectric layer thickness h are two adjustable geometric parameters.

corresponding fitness for the geometric parameters of P basic metaparticles.

The main objective of this paper was to control the interactions between 16 local waves produced by the basic metaparticles to achieve phase cancellation for a 10 dB RCS reduction in the superwide frequency band. However, this process is very challenging. PSO [36] together with (5) was used to optimize the side length L and layer thickness h of 16 basic metaparticles. In optimization, RCS reduction (σ_R) values at Q optimization frequencies sampled in a superwide frequency band needed to be evaluated. A cancellation error occurs when some frequencies have a very large σ_R value and others with a very small σ_R value. Therefore, we could not directly sum up the σ_R values at all of the optimization frequencies to evaluate the fitness. Thus, the fitness function is defined as

$$\text{fitness} = \sum_{i=1}^{Q} s(i) \tag{8}$$

and

$$s(i) = \begin{cases} 1, & \text{if } \sigma_R^i > -10 \text{ dB} \\ 0, & \text{if } \sigma_R^i \le -10 \text{ dB} \end{cases} \tag{9}$$

where σ_R^i is the RCS reduction under normal incidence at the ith frequency. The smaller the fitness is, the better is the RCS reduction.

The detailed flowchart of the OMEPC for superwideband RCS reduction is presented in Fig. 4. The initial side length of the basic metaparticle is a random value chosen from a uniform distribution between 1.2 and 7.6 mm. Layer thickness h is a discrete value chosen from 2, 4, and 6 mm. When 1000 iterations were finished, we got the optimal geometric parameters of 16 basic metaparticles for the metasurface with the lowest backward RCS in a desired superwide frequency band.

The optimized results of side length L and layer thickness h are listed in Table I. The predicted RCS reduction is shown in Fig. 5(a). In a superwide frequency band from 5.08 to 27.74 GHz, the RCS reductions are larger than 10 dB. Their corresponding reflection phases are shown in Fig. 5(b). For different frequencies, the basic metaparticles have different reflection phase responses, but they can always satisfy the phase cancellation condition for 10 dB RCS reduction depicted in (6) within 5.08–27.74 GHz. It is worth noticing that the phases of most (12 out of 16) metaparticles are very close

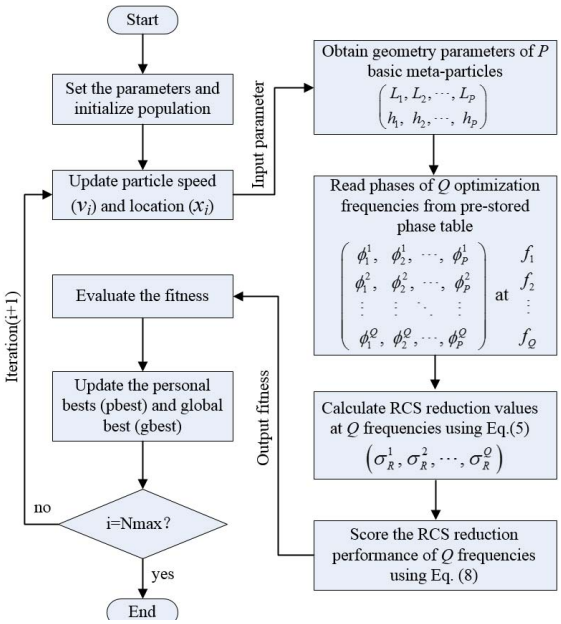

Fig. 4. Flowchart of the basic metaparticle optimization process for superwideband RCS reduction.

TABLE I
OPTIMIZED RESULTS OF 16 BASIC METAPARTICLES

Meta-particle:	**1**	**2**	**3**	**4**	**5**	**6**	**7**	**8**
***L* (mm)**	7.1	1.2	4.0	6.8	6.0	4.2	7.3	7.6
***h* (mm)**	4	6	4	4	2	2	4	2
Meta-particle:	**9**	**10**	**11**	**12**	**13**	**14**	**15**	**16**
***L* (mm)**	4.3	6.7	4.3	6.8	2.5	7.6	6.7	6.1
***h* (mm)**	2	6	6	4	6	2	2	6

at 4 GHz, leading to a low RCS reduction of only 0.6 dB. Compared with OPC and coding metamaterial, the advantage of this approach is that more basic metaparticles and variable phase differences between them greatly increase the ability for superwideband manipulation of EM waves and realizing superwideband phase cancellation.

C. Surface Metaparticle Layout

The metasurface consisted of these 16 basic metaparticles. According to (2) and (3), the scattering pattern $E^S(\theta, \varphi)$ in space is determined by the arrangement of the basic metaparticles, except for the backward direction ($\theta = 0, \varphi = 0$). We need to find the optimal metaparticle distribution with a lowest bistatic RCS in the superwide frequency band. The bistatic RCS reduction (σ_R^{Bi}) defined in [23] is described as

$$\sigma_R^{Bi} = \frac{\max(\text{Bistatic RCS with metasurface})}{\max(\text{Bistatic RCS without metasurface})}. \quad (10)$$

For a checkerboard surface with P basic tiles, the bistatic RCS reduction can be approximated by

$$\sigma_R^{Bi} = 10 \log \left[\frac{\max |\text{AF}(\theta, \varphi)|}{P} \right]^2. \quad (11)$$

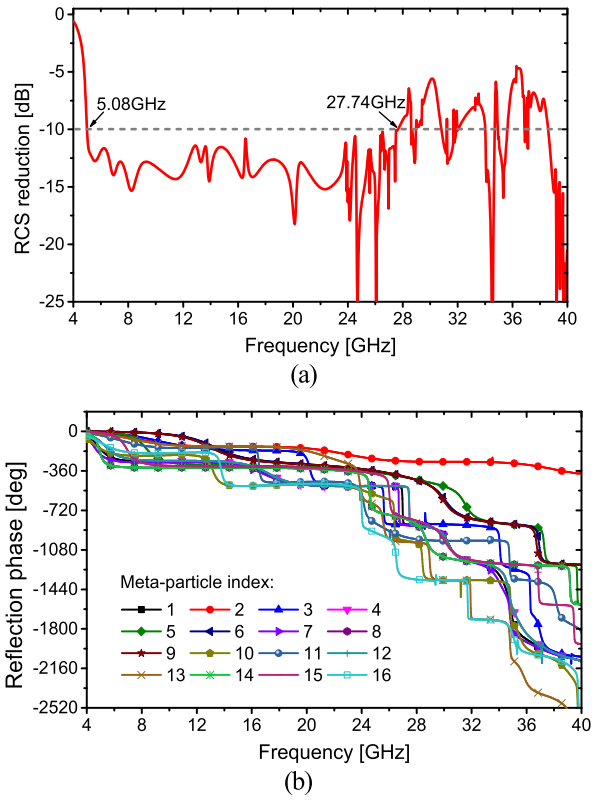

Fig. 5. Optimized results of RCS reduction. (a) Predicted monostatic RCS reduction. (b) Reflection phase of these 16 basic metaparticles.

The arithmetic mean of bistatic RCS reductions at $Q = 24$ frequency points from 5 to 28 GHz with an interval of 1 GHz are used to evaluate the figure of merit for bistatic scattering characteristics (FMB). Thus, FMB can be described as

$$\text{FMB} = \frac{20}{Q} \sum_{i=1}^{Q} \log \left[\frac{\max |\text{AF}_i(\theta, \varphi)|}{P} \right]. \quad (12)$$

The diffuse scattering of EM wave, which can effectively reduce the bistatic RCS, is caused by random metaparticle distribution through a certain computer-generated pseudorandom matrix [37]. In order to facilitate manufacturing of the metasurface, the tiles with the equal layer thickness are put together. After 500 random distributions were performed, an optimal surface metaparticle layout with minimum FMB is chosen to build the RCS reducer metasurface. The FMB value versus distribution index is plotted in Fig. 6. For the optimal distribution, the average of bistatic RCS reductions from 5 to 28 GHz is 7 dB. The optimal distribution of 16 basic metaparticles and the full structure of the metasurface are depicted in Fig. 7. To approximate the PBC used in the simulation, each tile is occupied by a subarray of 7×7 metaparticles. The model of the optimized RCS reducer metasurface has an overall dimension of 224×224 mm^2.

IV. SIMULATION AND MEASUREMENT

A. Simulated Results

A full structure of the metasurface was full-wave simulated by the transient solver of CST Microwave Studio. The RCS of

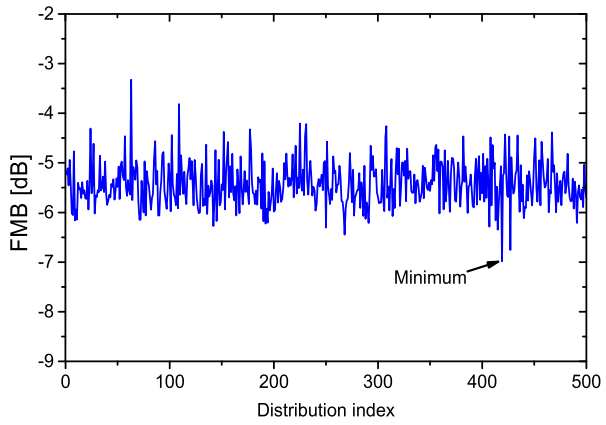

Fig. 6. Random process of FMB.

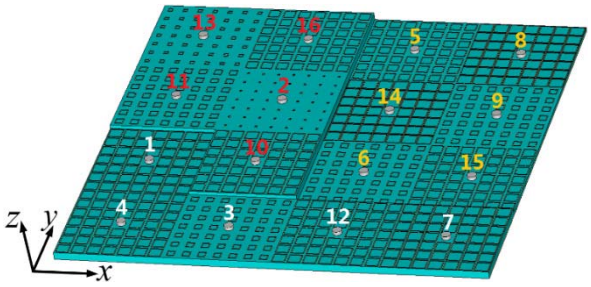

Fig. 7. Full model of the optimized RCS reducer metasurface. The inserted index is the metaparticle number shown in Table I.

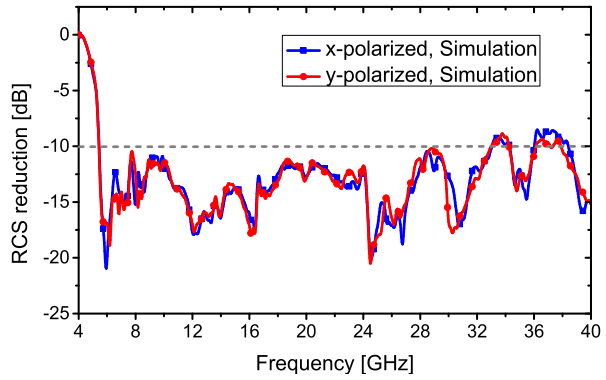

Fig. 8. Simulated RCS reduction versus frequency.

the metasurface normalized to that of an equal-sized PEC surface with a plane wave normally impinging is shown in Fig. 8. The metasurface can achieve the 10 dB RCS reduction in a superwide frequency band from 5.4 to 33.0 GHz with a ratio bandwidth of 6.11:1. The simulated results agree well with the predicted results in Section III. Both results imply that the proposed physical mechanism of OMEPC is able to greatly expand the bandwidth of RCS reduction. The slight difference between the predicted and simulated results is owing to the coupling between different metaparticles, which is neglected in theoretical calculation.

The 16 metaparticles of the metasurface present different phase responses, which is critical in disturbing the equiphase reflection. Due to the nonuniform distributions of the phase gradient between neighboring tiles, the specular reflections no longer dominate within the whole scattered waves. As a result, the metasurface generates a diffusion scattering pattern in the far field with the suppressed amplitude. The scattering patterns between the proposed metasurface and the equal-sized PEC surface under normal incidence are compared in Fig. 9 at 6, 12, and 24 GHz, respectively. The bistatic RCS of the metasurface is much lower than that of the equal-sized PEC surface. It is worth noting that the effective periodicity of the AF decreases as the frequency increases, leading to close concentrations of the scattering beams [34]. For different frequencies, the phase layout response of the metasurface is different, resulting in different diffusion scattering patterns.

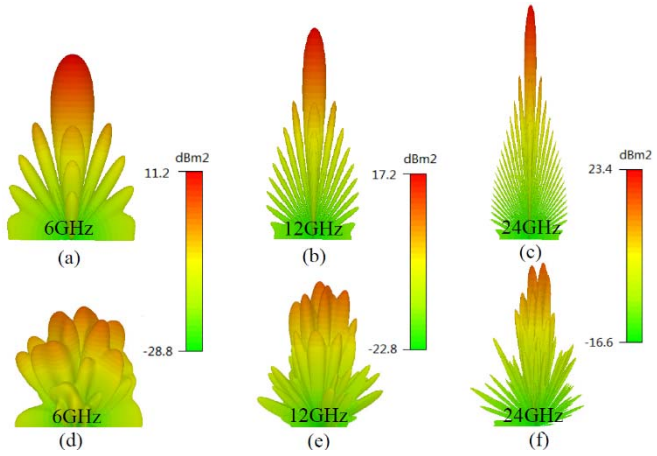

Fig. 9. Comparison of the bistatic scattering patterns between the proposed metasurface and equal-sized PEC surface under normal incidence at 6, 12, and 24 GHz, respectively. (a)–(c) For equal-sized PEC surface. (d)–(f) For the metasurface.

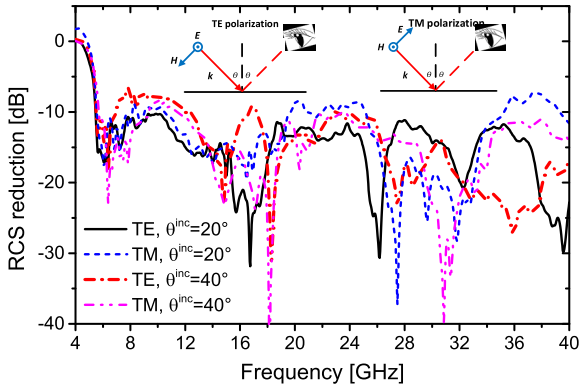

Fig. 10. RCS reductions in the specular direction under oblique incidence for TE and TM polarizations. TE/TM: direction of the electric/magnetic field is perpendicular to the plane of incidence.

In addition, the scattering properties of the metasurface under oblique incidences for both transverse-electric (TE) and transverse-magnetic (TM) polarizations are also provided in Fig.10. Significant RCS reduction is obtained from 5.5 to 40 GHz under wide-angle incidences for both polarizations. Simulation results illustrate the excellent performance of RCS reduction under oblique incidences.

B. Measured Results

To validate the predicted performance of the proposed metasurface, a sample of the metasurface was fabricated

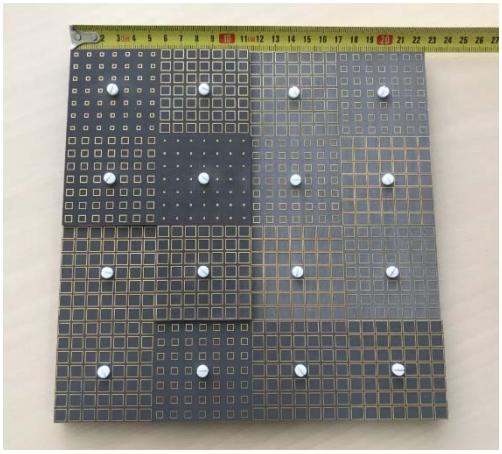

(a)

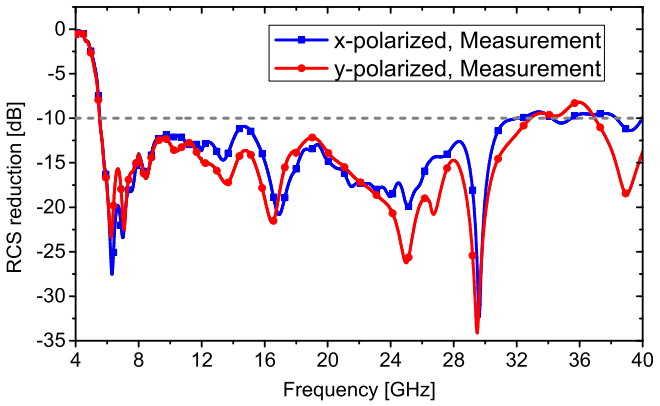

(b)

Fig. 11. Fabrication and measurement of the proposed RCS reducer metasurface. (a) Photograph of the fabricated metasurface. (b) Measured results of RCS reduction for the normal incidences.

and measured. The sample was manufactured using the printed circuit board technology. Three pieces of the metasurface board with different thicknesses were processed separately and then stitched together and fixed on the metal ground with Teflon bolts, as per our metasurface design. The dielectric substrate is polytetrafluoroethylene woven glass substrate with a dielectric constant $\varepsilon_r = 2.65$ (loss tangent $\tan\delta = 0.001$). The metal patches and ground are 0.035 mm thick copper layers. The diameter of the Teflon bolt is 3 mm and the dielectric constant is 2.1. A photograph of the fabricated sample is shown in Fig. 11(a). A high-precision RCS measurement was conducted using the compact antenna test range system of the Science and Technology on Electromagnetic Scattering Laboratory, Beijing, China. An equal-sized copper ground of the proposed metasurface is also measured as a reference. Fig. 11(b) shows the measured results of the RCS reductions versus frequency under normal incidence. The metasurface can realize an RCS reduction of larger than 8 dB in a superwide frequency band from 5.4 to 40 GHz with a ratio bandwidth of 7.4:1 for both x- and y-polarizations. The RCS reductions are larger than 10 dB from 5.5 to 32.3 GHz with a ratio bandwidth of 5.87:1. We note that the measurements agree well with the simulations shown in Fig. 8. The value deviations can be attributed to manufacturing and measurement error. Good phase cancellation is achieved in a superwide frequency band. A comparison between the previous studies and this paper is provided in Table II. Obviously, our work has an overwhelming advantage in the bandwidth expansion of RCS reduction. Overall, the bandwidth maximization for RCS reduction and diffusion scattering by the proposed metasurface based on OMEPC is confirmed.

TABLE II
COMPARISON OF OUR WORK AND PREVIOUS WORKS

Article	σ_R (dB)	OFB (GHz)	FBW (%)	RBW (f_H/f_L)
[22]	10	14.5-21.8	41	1.50:1
[23]	10	9.3-15.5	50	1.67:1
[25]	10	4.1-7.59	60	1.85:1
[26]	10	9.40-23.28	85	2.48:1
[27]	10	10.5-18	52.63	1.71:1
[32]	10	7.9-20.8	89.9	2.63:1
[33]	10	17-42	84.75	2.47:1
[30]	10	6.1-17.8	98	2.92:1
[28]	10	3.8-10.7	95	2.82:1
This Work	10	5.5-32.3	141.8	5.87:1
	8	5.4-40	152.4	7.4:1

σ_R: RCS reduction
OFB: Operating frequency band
FBW: The fractional bandwidth (FBW $= (f_H - f_L)/f_c$, $f_c = (f_H + f_L)/2$)
RBW: The ratio bandwidth (RBW $= f_H/f_L$)

V. CONCLUSION

A novel checkerboard metasurface based on OMEPC was designed, fabricated, and tested for superwideband RCS reduction. More basic metaparticles and variable phase differences between them greatly increase the ability to achieve phase cancellation. Interactions between multiple local waves produced by the basic metaparticles at multiple frequencies sampled in a superwide frequency band are manipulated and optimized simultaneously to achieve phase cancellation by field superposition principle and PSO algorithm. The metasurface can achieve more than 10 dB RCS reduction in a superwide frequency band ranging from 5.5 to 32.3 GHz with a ratio bandwidth of 5.87:1 under normal incidence for both x- and y-polarized waves. Furthermore, the RCS reduction is larger than 8 dB from 5.4 to 40 GHz with a ratio bandwidth of 7.4:1. The diffuse scattering of EM waves is caused by the random metaparticle distribution, leading to a low bistatic RCS simultaneously. The analysis, simulation, and test results show that the new physical mechanism, OMEPC, can effectively break the bandwidth constraints of traditional phase cancellation method and greatly expanding the bandwidth of RCS reduction.

REFERENCES

[1] T. J. Cui, W. X. Tang, X. M. Yang, Z. L. Mei, and W. X. Jiang, *Metamaterials: Beyond Crystals, Noncrystals, and Quasicrystals*, 1st ed. Boca Raton, FL, USA: CRC Press, 2016.

[2] D. R. Smith, J. B. Pendry, and M. C. K. Wiltshire, "Metamaterials and negative refractive index," *Science*, vol. 305, no. 5685, pp. 788–792, Aug. 2004.
[3] W. L. Barnes, A. Dereux, and T. W. Ebbesen, "Surface plasmon subwavelength optics," *Nature*, vol. 424, no. 6950, pp. 824–830, Aug. 2003.
[4] N. M. Litchinitser, A. I. Maimistov, I. R. Gabitov, R. Z. Sagdeev, and V. M. Shalaev, "Metamaterials: Electromagnetic enhancement at zero-index transition," *Opt. Lett.*, vol. 33, no. 20, pp. 2350–2352, Oct. 2008.
[5] A. Alu and N. Engheta, "Pairing an epsilon-negative slab with a mu-negative slab: Resonance, tunneling and transparency," *IEEE Trans. Antennas Propag.*, vol. 51, no. 10, pp. 2558–2571, Oct. 2003.
[6] J. B. Pendry, "Negative refraction makes a perfect lens," *Phys. Rev. Lett.*, vol. 85, no. 18, pp. 3966–3969, Oct. 2000.
[7] D. Schurig *et al.*, "Metamaterial electromagnetic cloak at microwave frequencies," *Science*, vol. 314, no. 5801, pp. 977–980, Oct. 2006.
[8] R. Liu, C. Ji, J. J. Mock, J. Y. Chin, T. J. Cui, and D. R. Smith, "Broadband ground-plane cloak," *Science*, vol. 323, no. 5912, pp. 366–369, Jan. 2009.
[9] H. F. Ma and T. J. Cui, "Three-dimensional broadband ground-plane cloak made of metamaterials," *Nature Commun.*, vol. 1, no. 3, Jun. 2010, Art. no. 21.
[10] A. R. Davoyan, W. Liu, A. E. Miroshnichenko, I. V. Shadrivov, Y. S. Kivshar, and S. I. Bozhevolnyi, "Mode transformation in waveguiding plasmonic structures," *Photon. Nanostruct.*, vol. 9, no. 3, pp. 207–212, Jul. 2011.
[11] J. Yin, X. Wan, Q. Zhang, and T. J. Cui, "Ultra wideband polarization-selective conversions of electromagnetic waves by metasurface under large-range incident angles," *Sci. Rep.*, vol. 5, Jul. 2015, Art. no. 12476.
[12] C. M. Watts, X. Liu, and W. J. Padilla, "Metamaterial electromagnetic wave absorbers," *Adv. Mater*, vol. 24, no. 23, pp. OP98–OP120, Jun. 2012.
[13] H. Yang, X.-Y. Cao, J. Gao, W. Li, Z. Yuan, and K. Shang, "Low RCS metamaterial absorber and extending bandwidth based on electromagnetic resonances," *Prog. Electromagn. Res. M*, vol. 33, pp. 31–44 Oct. 2013.
[14] M. Yoo, H. K. Kim, and S. Lim, "Angular- and polarization-insensitive metamaterial absorber using subwavelength unit cell in multilayer technology," *IEEE Antennas Wireless Propag. Lett.*, vol. 15, pp. 414–417, 2016.
[15] D. S. Lee, L. F. Gonzalez, K. Srinivas, D. Auld, and K. C. Wong, "Aerodynamic/RCS shape optimisation of unmanned aerial vehicles using hierarchical asynchronous parallel evolutionary algorithms," in *Proc. 24th AIAA Appl. Aerodyn. Conf., Fluid Dyn. Co-Located Conf.*, 2006, p. 3331.
[16] E. F. Knott, *Radar Cross Section Measurements*. New York, NY, USA: Springer, 2012.
[17] Y. Zhang *et al.*, "A multi-frequency multi-standard wideband fractional-*N* PLL with adaptive phase-noise cancellation for low-power short-range standards," *IEEE Trans. Microw. Theory Techn.*, vol. 64, no. 4, pp. 1133–1142, Apr. 2016.
[18] J. Hu, W. Zhou, Y. Fu, X. Li, and N. Jing, "Uniform rotational motion compensation for ISAR based on phase cancellation," *IEEE Geosci. Remote Sens. Lett.*, vol. 8, no. 4, pp. 636–640, Jul. 2011.
[19] K. A. Wear, "The effect of phase cancellation on estimates of calcaneal broadband ultrasound attenuation *in vivo*," *IEEE Trans. Ultrason., Ferroelectr., Freq. Control*, vol. 54, no. 7, pp. 1352–1359, Jul. 2007.
[20] J. Suarez and P. R. Prucnal, "System-level performance and characterization of counter-phase optical interference cancellation," *J. Lightw. Technol.*, vol. 28, no. 12, pp. 1821–1831, Sep. 15, 2010.
[21] M. Paquay, J. C. Iriarte, I. Ederra, R. Gonzalo, and P. D. Maagt, "Thin AMC structure for radar cross-section reduction," *IEEE Trans. Antennas Propag.*, vol. 55, no. 12, pp. 3630–3638, Dec. 2007.
[22] J. C. I. Galarregui, A. T. Pereda, J. L. M. de Falcón, I. Ederra, R. Gonzalo, and P. de Maagt, "Broadband radar cross-section reduction using AMC technology," *IEEE Trans. Antennas Propag.*, vol. 61, no. 12, pp. 6136–6143, Dec. 2013.
[23] A. Edalati and K. Sarabandi, "Wideband, wide angle, polarization independent RCS reduction using nonabsorptive miniaturized-element frequency selective surfaces," *IEEE Trans. Antennas Propag.*, vol. 62, no. 2, pp. 747–754, Sep. 2014.
[24] Y. Zheng, J. Gao, X. Cao, Z. Yuan, and H. Yang, "Wideband RCS reduction of a microstrip antenna using artificial magnetic conductor structures," *IEEE Antennas Wireless Propag. Lett.*, vol. 14, pp. 1582–1585, 2015.
[25] W. Chen, C. A. Balanis, and C. R. Birtcher, "Checkerboard EBG surfaces for wideband radar cross section reduction," *IEEE Trans. Antennas Propag.*, vol. 63, no. 6, pp. 2636–2645, Jun. 2015.
[26] S. H. Esmaeli and S. H. Sedighy, "Wideband radar cross-section reduction by AMC," *Electron. Lett.*, vol. 52, no. 1, pp. 70–71, Aug. 2016.
[27] W. Pan *et al.*, "Combining the absorptive and radiative loss in metasurfaces for multi-spectral shaping of the electromagnetic scattering," *Sci. Rep.*, vol. 6, Feb. 2016, Art. no. 21462.
[28] M. J. Haji-Ahmadi, V. Nayyeri, M. Soleimani, and O. M. Ramahi, "Pixelated checkerboard metasurface for ultra-wideband radar cross section reduction," *Sci. Rep.*, vol. 7, no. 1, Sep. 2017, Art. no. 11437.
[29] Y. Jia, Y. Liu, Y. J. Guo, K. Li, and S.-X. Gong, "Broadband polarization rotation reflective surfaces and their applications to RCS reduction," *IEEE Trans. Antennas Propag.*, vol. 64, no. 1, pp. 179–188, Jan. 2016.
[30] Y. Jia, Y. Liu, Y. J. Guo, K. Li, and S. Gong, "A dual-patch polarization rotation reflective surface and its application to ultra-wideband RCS reduction," *IEEE Trans. Antennas Propag.*, vol. 65, no. 6, pp. 3291–3295, Jun. 2017.
[31] T. J. Cui, M. Q. Qi, X. Wan, J. Zhao, and Q. Cheng, "Coding metamaterials, digital metamaterials and programmable metamaterials," *Light Sci. Appl.*, vol. 3, no. 10, Jul. 2014, Art. no. e218.
[32] P. Su, Y. Zhao, S. Jia, W. Shi, and H. Wang, "An ultra-wideband and polarization-independent metasurface for RCS reduction," *Sci. Rep.*, vol. 6, Feb. 2016, Art. no. 20387.
[33] H. Sun *et al.*, "Broadband and broad-angle polarization-independent metasurface for radar cross section reduction," *Sci. Rep.*, vol. 7, Jan. 2017, Art. no. 40782.
[34] C. A. Balanis, *Antenna Theory: Analysis and Design*, 3rd ed. New York, NY, USA: Wiley 2005.
[35] J. Su *et al.*, "Ultra-wideband, wide angle and polarization-insensitive specular reflection reduction by metasurface based on parameter-adjustable meta-atoms," *Sci. Rep.*, vol. 7, Feb. 2017, Art. no. 42283.
[36] D. W. Boeringer and D. H. Werner, "Particle swarm optimization versus genetic algorithms for phased array synthesis," *IEEE Trans. Antennas Propag.*, vol. 52, no. 3, pp. 771–779, Mar. 2004.
[37] L. H. Gao *et al.*, "Broadband diffusion of terahertz waves by multi-bit coding metasurfaces," *Light Sci. Appl.*, vol. 4, no. 9, p. e324, Sep. 2015.

Jianxun Su received the B.S. degree in electronic information engineering from the Taiyuan University of Technology, Taiyuan, China, in 2006, the M.S. degree in electromagnetic field and microwave technology from the Communication University of China, Beijing, China, in 2008, and the Ph.D. degree in electromagnetic field and microwave technology from the Beijing Institute of Technology, Beijing, in 2011.

From 2012 to 2014, he was with China Electronics Technology Group Corporation, Beijing, where he was involved in phased-array system research. He is currently an Associate Researcher with the School of Information Engineering, Communication University of China and the Science and Technology on Electromagnetic Scattering Laboratory, Beijing. His current research interests include integral equation method, metamaterial, array antenna, and radar target characteristics.

Yao Lu received the B.Eng. degree in communication engineering from the Communication University of China, Beijing, China, in 2015, where she is currently pursuing the M.S.E.E. degree.

Her current research interests include AMC structures, metasurface, and RCS reduction.

Jiayi Liu received the B.Eng. degree in communication engineering from the Communication University of China, Beijing, China, in 2017, where she is currently pursuing the M.S. degree.

Her current research interests include metamaterial, corner reflector, and electromagnetic wave manipulation.

Yaoqing (Lamar) Yang (S'02–M'09–SM'09) received the B.S. degree in electrical engineering from Beijing Jiaotong University, Beijing, China, in 1983, the M.S. degree in electrical engineering from the Beijing Broadcast Institute, Beijing, in 1986, and the Ph.D. degree in wireless communications and networks from the University of Texas (UT) at Austin, Austin, TX, USA, in 2006.

From 2003 to 2005, he was a Teaching Assistant with UT at Austin, and from 1999 to 2002, he was also a Research Assistant sponsored by the Advanced Research Program. From 1986 to 1997, he was a Lecturer with the Beijing Broadcast Institute. He is currently an Associate Professor with the Department of Electrical and Computer Engineering, University of Nebraska–Lincoln (UNL), Lincoln, NE, USA, where he has held a tenure-track faculty position in 2006. His current research interests include wireless communications, radio propagations, and statistical signal processing.

Dr. Yang served as a Technical Program Committee Member for many years for numerous top-ranked conferences, including IEEE GLOBECOM, ICC, VTC, WCNC, and MSWiM. He was a recipient of the Kleinkauf New Faculty Teaching Award in 2009 and the Holling Family Distinguished Teaching Award in 2011. He served as a reviewer for the IEEE TRANSACTIONS ON WIRELESS COMMUNICATIONS, the IEEE TRANSACTIONS ON VEHICULAR TECHNOLOGY, IEEE TRANSACTIONS ON CIRCUITS AND SYSTEMS FOR VIDEO TECHNOLOGY, and IEEE COMMUNICATIONS LETTERS.

Zengrui Li (M'11) received the B.S. degree in communication and information system from Beijing Jiaotong University, Beijing, China, in 1984, the M.S. degree in electrical engineering from the Beijing Broadcast Institute, Beijing, in 1987, and the Ph.D. degree in electrical engineering from Beijing Jiaotong University in 2009.

From 2004 to 2005, he was with Yokohama National University, Yokohama, Japan. He is currently a Professor with the Communication University of China, Beijing. His current research interests include finite-difference time-domain methods, electromagnetic scattering, metamaterials, and antennas.

Dr. Li is a Senior Member of the Chinese Institute of Electronics.

Jiming Song (S'92–M'95–SM'99–F'14) received the B.S. and M.S. degrees in physics from Nanjing University, Nanjing, China, in 1983 and 1988, respectively, and the Ph.D. degree in electrical engineering from Michigan State University, East Lansing, MI, USA, in 1993.

From 1993 to 2000, he was a Post-Doctoral Research Associate, a Research Scientist, and a Visiting Assistant Professor with the University of Illinois at Urbana–Champaign, Champaign, IL, USA. From 1996 to 2000, he was a Part-Time Research Scientist with SAIC-Champaign, (formerly Demaco, Inc.), Champaign. He was a Principal Staff Engineer/Scientist with Semiconductor Products Sector of Motorola, Tempe, AZ, USA. In 2002, he joined the Department of Electrical and Computer Engineering, Iowa State University, Ames, IA, USA, as an Assistant Professor, where he is currently a Professor. He is also a Visiting Professor with the School of Information Engineering, Communication University of China, Beijing, China. He has authored the Fast Illinois Solver Code. His current research interests include the modeling and simulations of interconnects on lossy silicon and RF components, electromagnetic wave scattering using fast algorithms, the wave propagation in metamaterials, acoustic and elastic wave propagation and nondestructive evaluation, and transient electromagnetic field.

Dr. Song is an ACES Fellow. He was selected as a National Research Council/Air Force Summer Faculty Fellow in 2004 and 2005. He was a recipient of the NSF Career Award in 2006. He is an Associate Editor of IEEE ANTENNAS AND WIRELESS PROPAGATION LETTERS and *ACES Express*.